Cell Reports, Volume *31*

Supplemental Information

The PD-1 Pathway Regulates Development and Function of Memory CD8$^+$ T Cells following Respiratory Viral Infection

Kristen E. Pauken, Jernej Godec, Pamela M. Odorizzi, Keturah E. Brown, Kathleen B. Yates, Shin Foong Ngiow, Kelly P. Burke, Seth Maleri, Shannon M. Grande, Loise M. Francisco, Mohammed-Alkhatim Ali, Sabrina Imam, Gordon J. Freeman, W. Nicholas Haining, E. John Wherry, and Arlene H. Sharpe

Figure S1

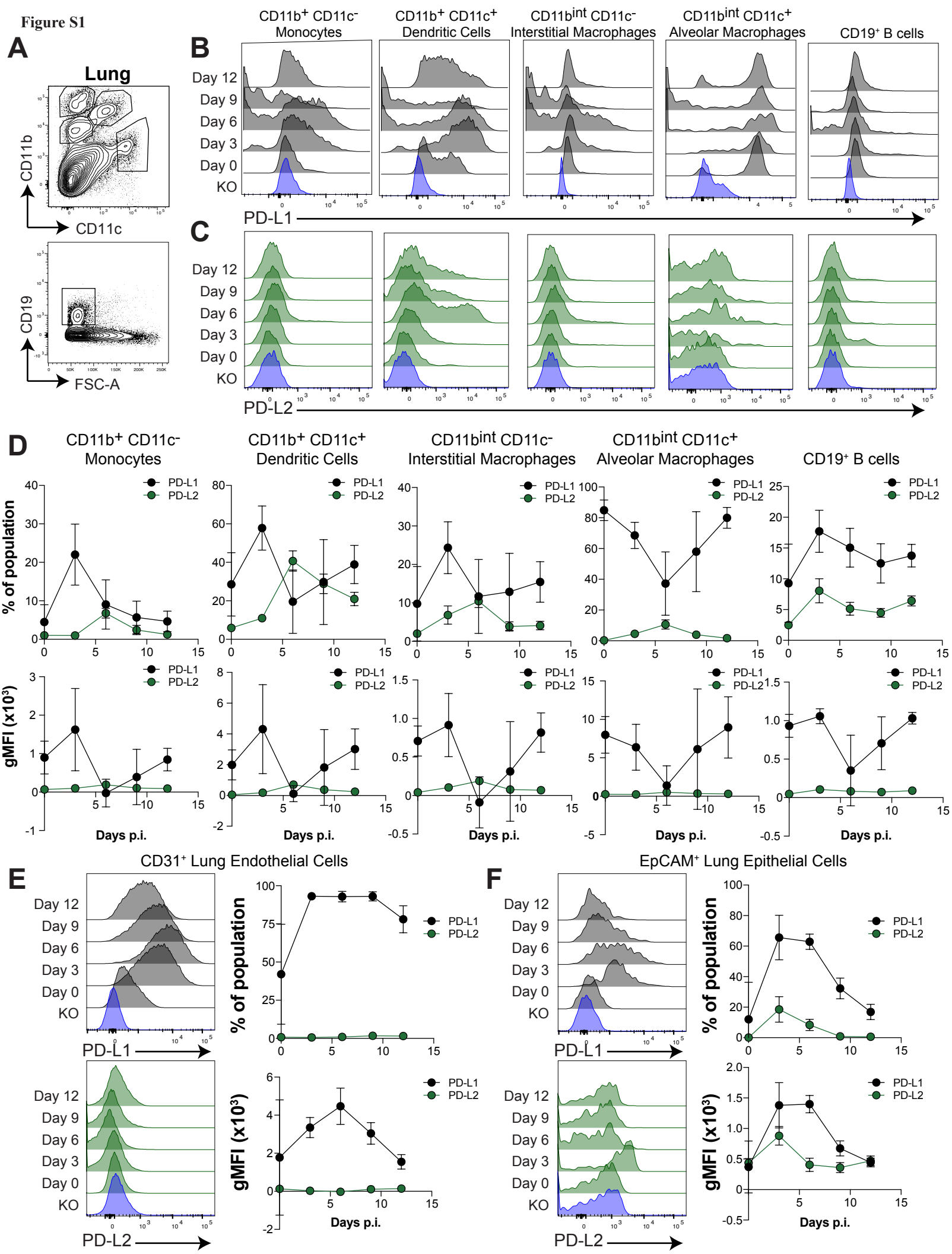
A
Lung
CD11b
CD11c
CD19
FSC-A
B
CD11b+ CD11c- Monocytes
CD11b+ CD11c+ Dendritic Cells
CD11bint CD11c- Interstitial Macrophages
CD11bint CD11c+ Alveolar Macrophages
CD19+ B cells
Day 12
Day 9
Day 6
Day 3
Day 0
KO
PD-L1
C
PD-L2
D
% of population
gMFI (x10³)
PD-L1
PD-L2
Days p.i.
E
CD31+ Lung Endothelial Cells
F
EpCAM+ Lung Epithelial Cells

Figure S1, related to Figure 1. Expression of PD-L1 and PD-L2 on lung cell subsets following influenza infection. Phenotypic analysis of PD-L1 and PD-L2 expression on cell subsets following X31-GP33 infection. (A) Gating strategy used for lung myeloid subsets and B cells in (B - D). Expression of PD-L1 (black) and PD-L2 (green) in lung myeloid subsets and B cells (B - D), endothelial cells (E), and epithelial cells (F) following primary X31-GP33 influenza infection. Blue histogram indicates KO control. Representative flow cytometry histograms and summary data of 5 mice per group shown for each population. Data are represented as mean ± SEM. Abbreviations used include: MFI=mean fluorescence intensity, p.i.=post-infection.

Figure S2

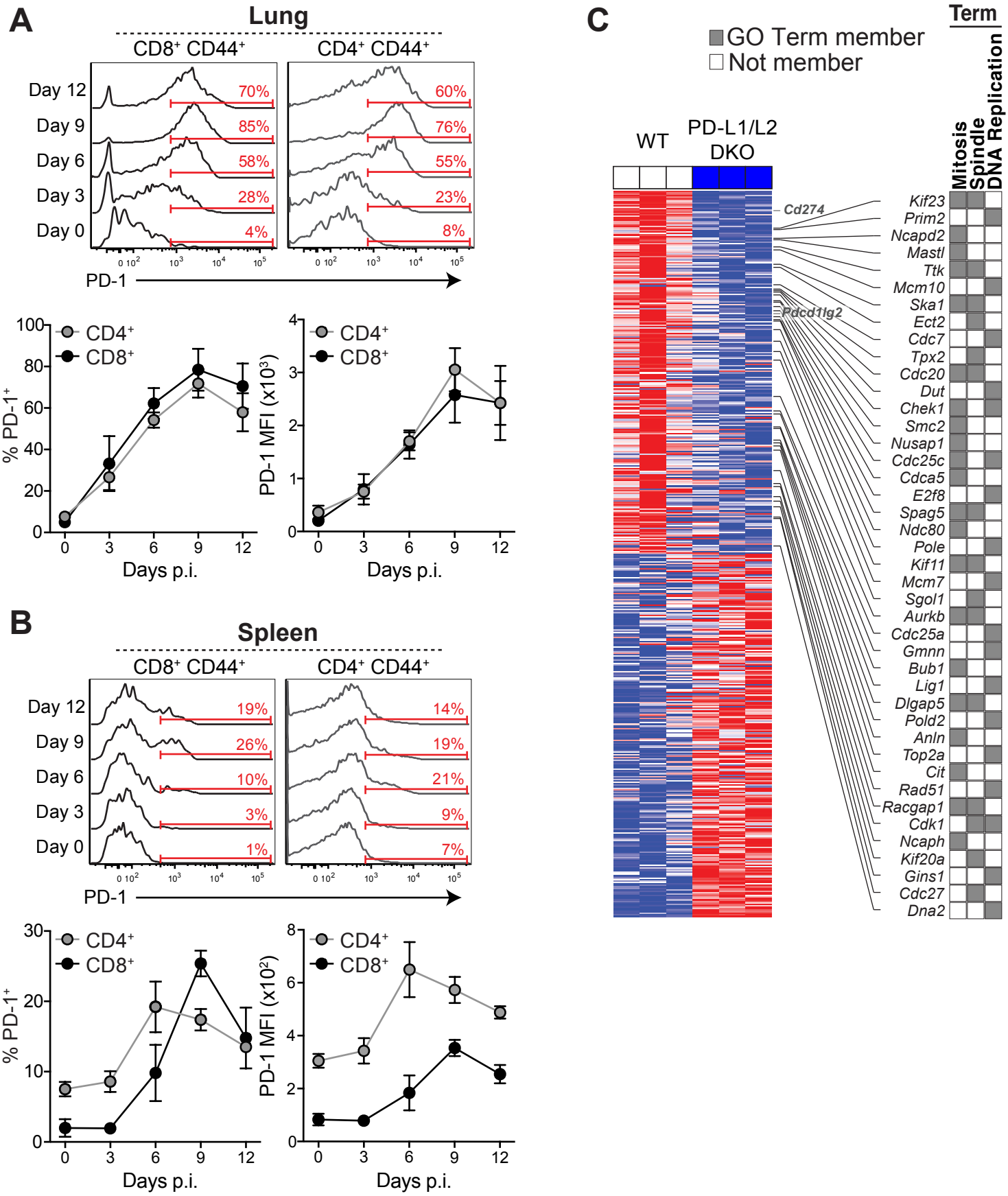
A
Lung
CD8⁺ CD44⁺
CD4⁺ CD44⁺
Day 12
Day 9
Day 6
Day 3
Day 0
70%
85%
58%
28%
4%
60%
76%
55%
23%
8%
PD-1
CD4⁺
CD8⁺
% PD-1⁺
PD-1 MFI (x10³)
Days p.i.
B
Spleen
19%
26%
10%
3%
1%
14%
19%
21%
9%
7%
PD-1 MFI (x10²)
C
GO Term member
Not member
GO Term
Mitosis
Spindle
DNA Replication
WT
PD-L1/L2 DKO
Cd274
Pdcd1lg2
Kif23
Prim2
Ncapd2
Mastl
Ttk
Mcm10
Ska1
Ect2
Cdc7
Tpx2
Cdc20
Dut
Chek1
Smc2
Nusap1
Cdc25c
Cdca5
E2f8
Spag5
Ndc80
Pole
Kif11
Mcm7
Sgol1
Aurkb
Cdc25a
Gmnn
Bub1
Lig1
Dlgap5
Pold2
Anln
Top2a
Cit
Rad51
Racgap1
Cdk1
Ncaph
Kif20a
Gins1
Cdc27
Dna2

Figure S2, related to Figure 1. Expression of PD-1 on lung cell subsets following influenza infection and gene expression in PD-1 pathway deficient mice. (A, B) WT mice were infected with X31-GP33 influenza and antigen-experienced $CD44^+$ $CD8^+$ and $CD44^+$ $CD4^+$ T cells were analyzed for their expression of PD-1 before (d0) and after (d3-d12) infection in the lung (A) and spleen (B). Representative plots (top) and summarized frequencies (of parent gate) and MFI shown (bottom). $CD4^+$ T cells are shown in grey, $CD8^+$ T cells are shown in black. Representative flow cytometry histograms and summary of data of 5 mice per group shown for each population. These data are from one representative experiment with mean ± SD. Data from key time points (days 0, 8) are representative of 2-3 independent experiments with 2-7 mice per group. (C) Top 250 differentially expressed genes in subdominant-epitope (D^bGP_{33-41} and $D^bPA_{224-233}$) specific T cells from WT and PD-L1/PD-L2 DKO mice ranked by signal-to-noise values following filtration to top 10% of genes with highest mean absolute deviation across samples. Membership of genes in the three representative GO terms is shown on the right. Abbreviations used include: MFI=mean fluorescence intensity, p.i.=post-infection, GO=Gene Ontogeny.

Figure S3

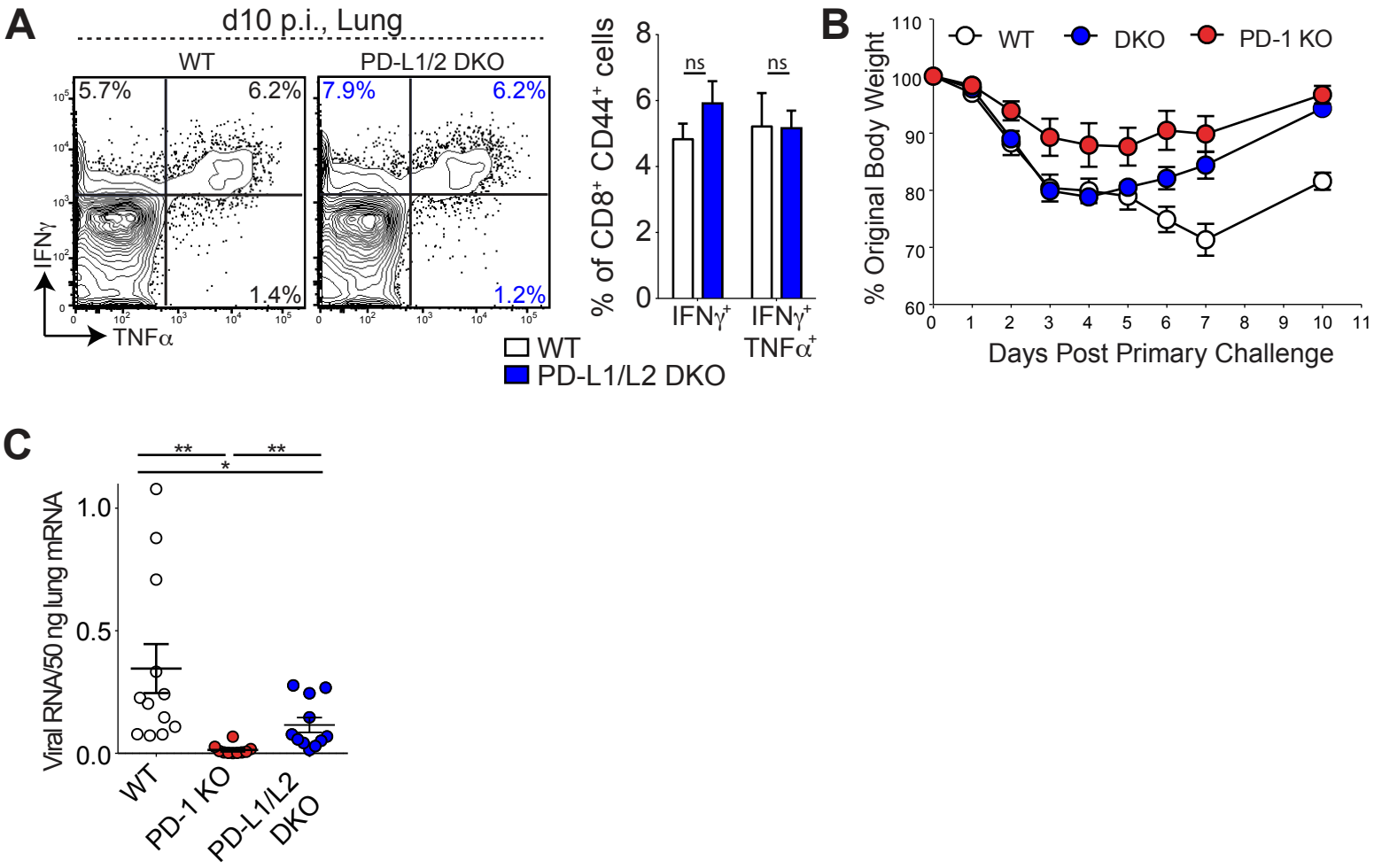
A
d10 p.i., Lung
WT
PD-L1/2 DKO
5.7%
6.2%
1.4%
7.9%
6.2%
1.2%
IFNγ
TNFα
% of CD8+ CD44+ cells
ns
ns
IFNγ+
IFNγ+ TNFα+
WT
PD-L1/L2 DKO
B
WT
DKO
PD-1 KO
% Original Body Weight
Days Post Primary Challenge
C
Viral RNA/50 ng lung mRNA
**
**
*
WT
PD-1 KO
PD-L1/L2 DKO

Figure S3, related to Figure 1. PD-1 deficient mice show enhanced disease control following primary X31-GP33 infection. (A) Representative plots of intracellular cytokine staining for IFN-γ and TNF-α production in lung $CD8^+$ T cells on d10 p.i. following *ex vivo* stimulation with $NP_{366-374}$ peptide. Representative plots gated on $CD8^+$ $CD44^+$ T cells (left) and summary of percent responding cells (right) from 5 mice per group. (B) Weight loss in WT, PD-1 KO, and PD-L1/L2 DKO mice following primary infection with X31-GP33. (C) Influenza viral titers in the lung of WT, PD-1 KO, and PD-L1/L2 DKO mice at d7 p.i. Data are representative of 2-3 independent experiments with 3-5 mice per experiment. Data are represented as mean ± SEM. Significance was assessed using Student's t-test; ns = not significant $P > 0.05$, $*P < 0.05$, $**P < 0.01$. Abbreviations used include: p.i.=post-infection.

Figure S4

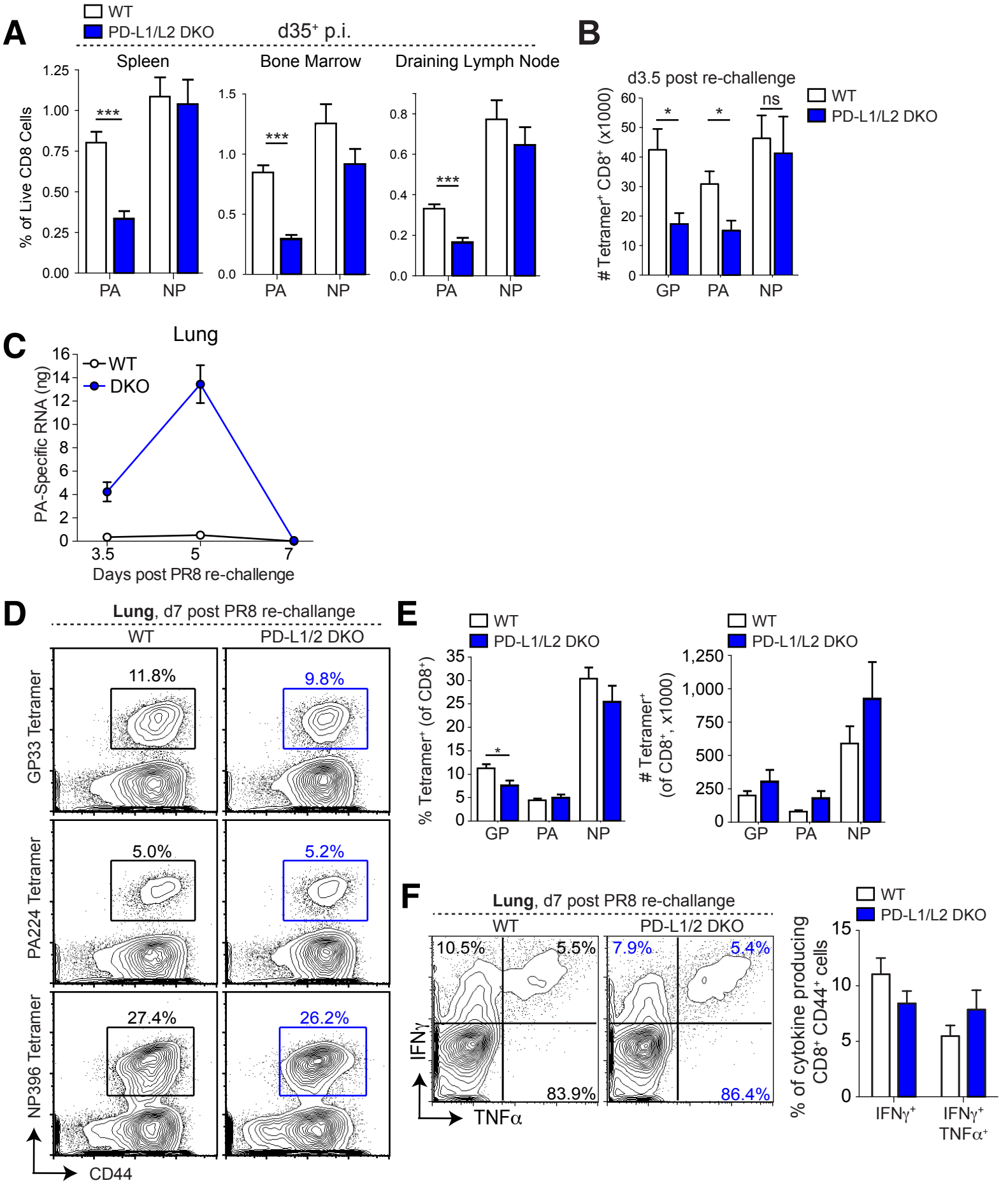
A
WT
PD-L1/L2 DKO
d35⁺ p.i.
Spleen
Bone Marrow
Draining Lymph Node
% of Live CD8 Cells
PA
NP
B
d3.5 post re-challenge
Tetramer⁺ CD8⁺ (x1000)
GP
PA
NP
ns
C
Lung
WT
DKO
PA-Specific RNA (ng)
Days post PR8 re-challenge
D
Lung, d7 post PR8 re-challange
WT
PD-L1/2 DKO
GP33 Tetramer
PA224 Tetramer
NP396 Tetramer
CD44
11.8%
9.8%
5.0%
5.2%
27.4%
26.2%
E
% Tetramer⁺ (of CD8⁺)
# Tetramer⁺ (of CD8⁺, x1000)
F
Lung, d7 post PR8 re-challange
IFNγ
TNFα
10.5%
5.5%
83.9%
7.9%
5.4%
86.4%
% of cytokine producing CD8⁺ CD44⁺ cells
IFNγ⁺
IFNγ⁺ TNFα⁺

Figure S4, related to Figure 2. Influenza-specific $CD8^+$ T cell numbers normalize at day 7 after secondary PR8-GP33 infection. (A) Summary of frequencies of memory $CD8^+$ T cells specific for influenza epitopes in the spleen (left), bone marrow (middle) and lung draining LN (right) in WT and PD-L1/PD-L2 DKO mice at $d35^+$ p.i. following primary X31-GP33 infection. (B) Summary of numbers of indicated $tetramer^+$ $CD8^+$ T cells in the lungs of WT and PD-L1/L2 DKO mice at d3.5 post-re-challenge with PR8-GP33. (C) Kinetics of viral clearance in WT and PD-L1/L2 DKO mice following secondary infection with PR8-GP33, 35 days following primary X31-GP33 infection. (D) Representative plots showing the frequencies of $D^bGP_{33\text{-}41}{}^+$ (upper), $D^bPA_{224\text{-}233}{}^+$ (middle) and $D^bNP_{366\text{-}374}{}^+$ (lower) $CD8^+$ T cells in the lungs of X31-GP33 immune WT and PD-L1/L2 DKO mice on d7 post-rechallenge with PR8-GP33. (E) Summary of mice shown in (D) indicating frequencies (left) and numbers (right) of $CD8^+$ T cells specific for influenza epitopes in lung of WT and PD-L1/L2 DKO mice on d7 post-rechallenge with PR8-GP33. (F) Representative plots for IFNγ and TNFα production in lung $CD8^+$ T cells from (D) and (E) stimulated *ex vivo* with $NP_{366\text{-}374}$ peptide (left). Fraction of responding cells summarized (right). Data are representative of 2-4 independent experiments with 4-5 mice per experiment. Data are represented as mean ± SEM. Significance was assessed using Student's t-test; $^*P < 0.05$, $^{***}P < 0.001$. Abbreviations used include: GP=$D^bGP_{33\text{-}41}$ tetramer, PA=$D^bPA_{224\text{-}233}$ tetramer, NP=$D^bNP_{366\text{-}374}$ tetramer.

Figure S5

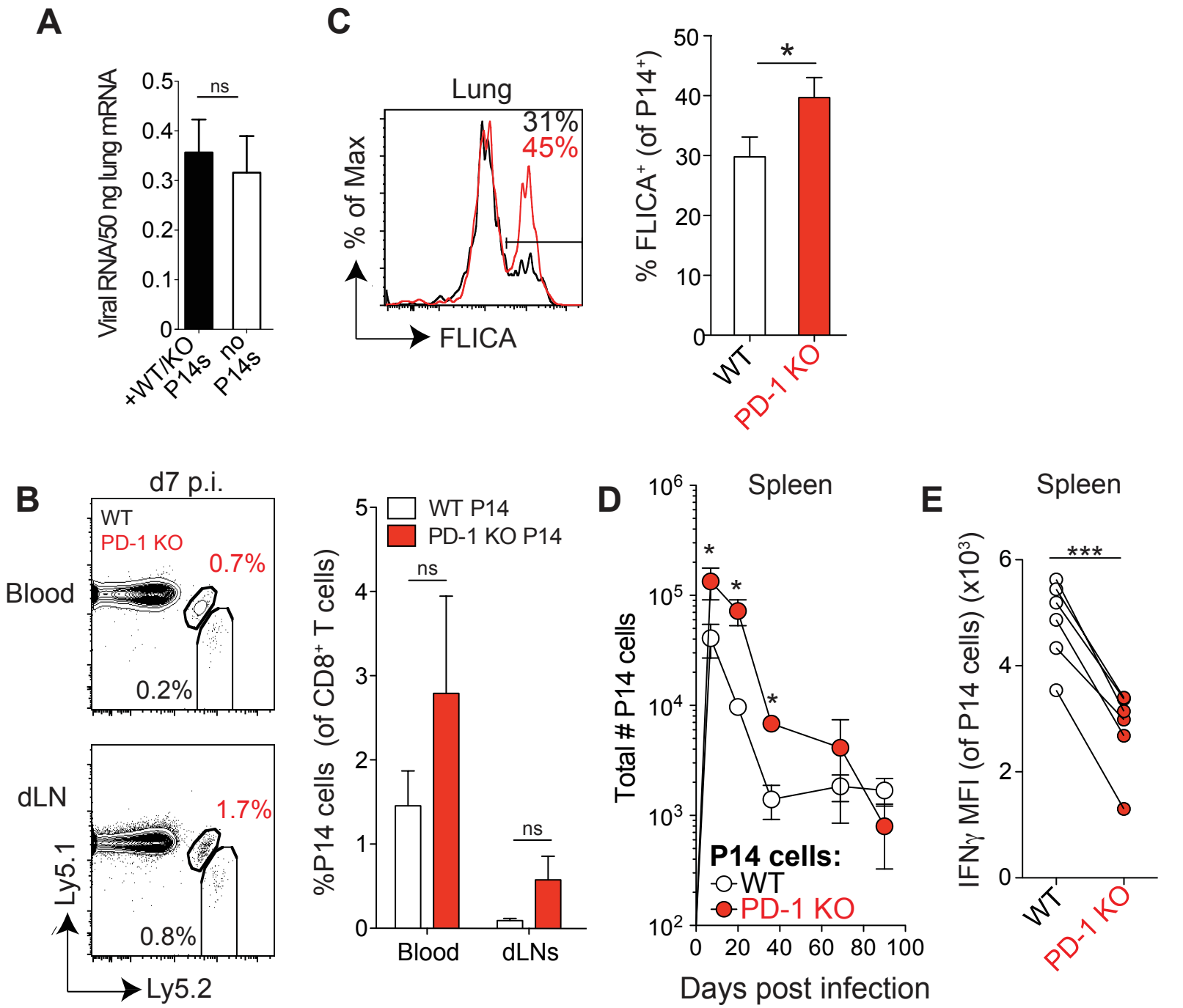
A
Viral RNA/50 ng lung mRNA
0.5
0.4
0.3
0.2
0.1
0
ns
+WT/KO P14s
no P14s
C
Lung
31%
45%
% of Max
FLICA
% FLICA+ (of P14+)
50
40
30
20
10
0
*
WT
PD-1 KO
B
d7 p.i.
WT
PD-1 KO
Blood
0.7%
0.2%
dLN
1.7%
0.8%
Ly5.1
Ly5.2
%P14 cells (of CD8+ T cells)
WT P14
PD-1 KO P14
ns
ns
Blood
dLNs
D
Spleen
Total # P14 cells
P14 cells:
WT
PD-1 KO
Days post infection
E
Spleen
IFNγ MFI (of P14 cells) (x10³)
***
WT
PD-1 KO

Figure S5, related to Figure 3. PD-1 controls $CD8^+$ T cell functions in a cell-intrinsic manner. (A) Quantification of viral load d8 after X31-GP33 infection in WT mice compared to WT mice that received a 50:50 mixture of WT and PD-1 KO P14 cells. (B) Representative plots (left) showing frequencies of WT and PD-1 KO P14 cells in indicated organs at d7 after X31-GP33 infection. Numbers indicate frequency of P14 cells as a percent of $CD8^+$ T cells. Summary of frequencies is shown on the right. (C) Flow cytometric analysis of active caspase by FLICA staining of lung WT and PD-1 KO P14 T cells on d8 p.i. Numbers indicate fraction of P14 cells positive for FLICA staining based on unstained controls. Representative histogram shown (left) and summary of frequencies of $FLICA^+$ cells shown (right). (D) Longitudinal analysis of WT and PD-1 KO P14 absolute cell numbers in the spleen during primary X31-GP33 infection. (E) Summary of MFI of WT and PD-1 KO P14 cell IFN-γ expression on $d60^+$ p.i. with X31-GP33 following *ex vivo* stimulation with GP_{33-41} peptide. Data are representative of 3 independent experiments with 4-5 mice per group. Data are represented as mean ± SEM. Significance was assessed using Student's t-test; $*P < 0.05$, $*** P < 0.001$. Abbreviations used include: MFI=mean fluorescence intensity.

Figure S6

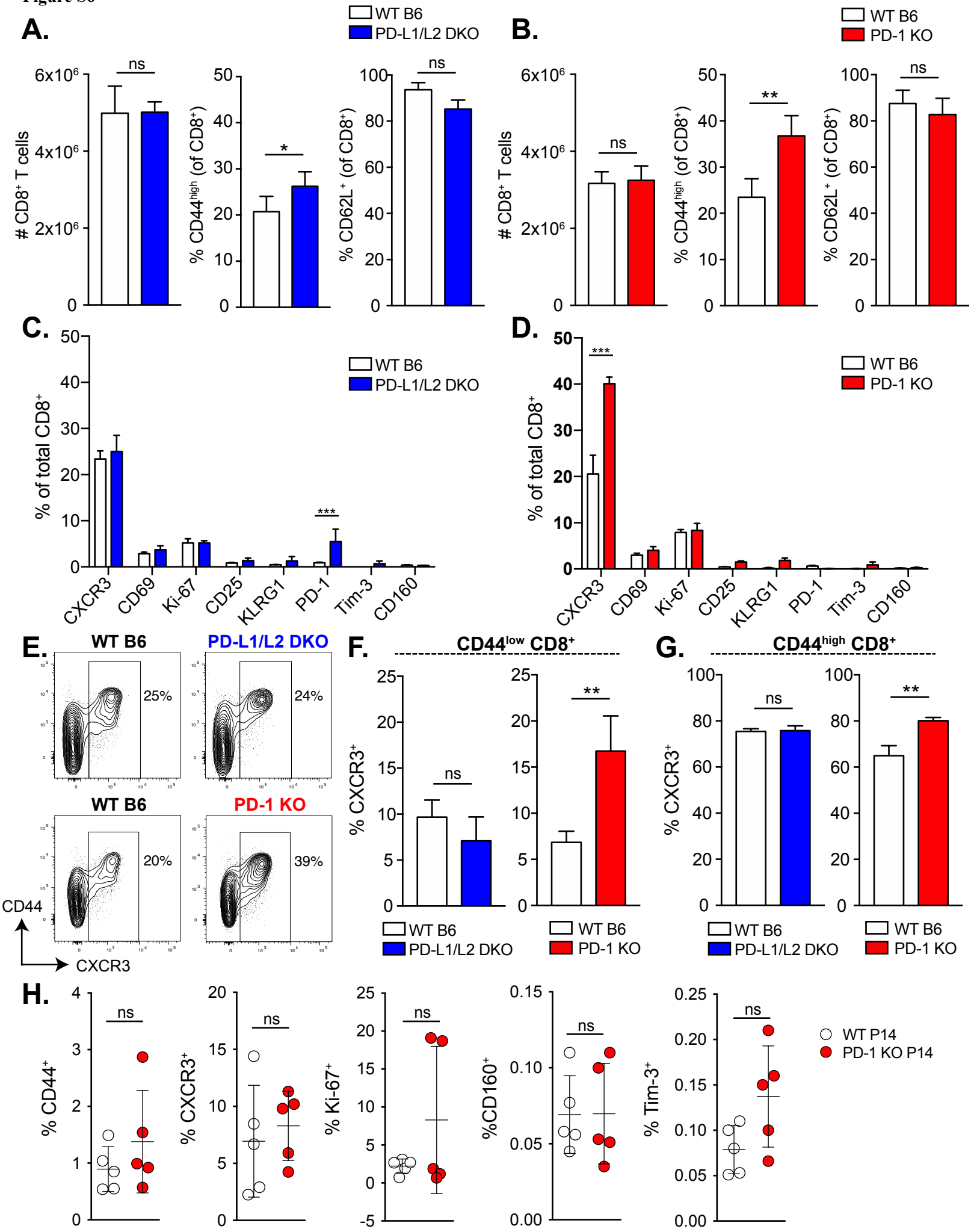
A.
WT B6
PD-L1/L2 DKO
CD8+ T cells
% CD44high (of CD8+)
% CD62L+ (of CD8+)
ns
*
B.
WT B6
PD-1 KO
**
C.
% of total CD8+
***
CXCR3
CD69
Ki-67
CD25
KLRG1
PD-1
Tim-3
CD160
D.
E.
WT B6
PD-L1/L2 DKO
25%
24%
WT B6
PD-1 KO
20%
39%
CD44
CXCR3
F.
CD44low CD8+
% CXCR3+
G.
CD44high CD8+
H.
% CD44+
% CXCR3+
% Ki-67+
%CD160+
% Tim-3+
WT P14
PD-1 KO P14

Figure S6, related to Figure 3. Phenotypic characterization of $CD8^+$ T cells in the steady state in naïve PD-1 KO, PD-L1/L2 DKO, and PD-1 KO P14 mice compared to WT. (A, B) Number of $CD8^+$ T cells (left), frequency of $CD44^{high}$ cells of the $CD8^+$ T cell population (middle), and frequency of $CD62L^+$ cells of the $CD8^+$ T cell population (right) in the spleen of uninfected 8-12 week old WT and PD-L1/L2 DKO mice (A) or WT and PD-1 KO mice (B). (C, D) Frequency of $CD8^+$ T cells in the spleen of the WT vs. PD-L1/L2 DKO (C) and PD-1 KO (D) shown in (A) and (B) that are positive for the indicated markers. (E) Representative flow cytometry contour plots showing CD44 and CXCR3 expression on $CD8^+$ T cells in spleens from WT, PD-L1/L2 DKO, and PD-1 KO mice shown in (A)-(D). (F, G) Quantification of the frequency $CD8^+$ $CD44^{low}$ (F) or $CD44^{high}$ cells (G) expressing CXCR3 in the spleen of WT and PD-L1/L2 DKO mice (left) or WT and PD-1 KO mice (right). (H) Frequency of P14 cells in the peripheral blood of intact WT or PD-1 KO P14 mice that are positive for the indicated markers. Data are representative of 2 independent experiments with 4-6 mice per group. Data are represented as mean ± SEM. Significance was assessed using unpaired Student's t-test in (A), (B), (F), (G), and (H), and 2 way ANOVA using multiple comparisons (Sidak's) post-test for (C) and (D); $^{**}P < 0.01$, $^{***} P < 0.001$.